

# Time-Lag Effects in Parker's Dynamo

M. Yu. Reshetnyak

*Schmidt Institute of Physics of the Earth, Russian Academy of Sciences,  
Bol'shaya Gruzinskaya ul. 10, Moscow, 123810 Russia*

Received 2010; in final form, April 2, 2010

**Abstract**—The effects of a time lag in the magnetic quenching of the  $\alpha$  effect is considered for an oscillating magnetic field in a Parker dynamo. The hypothesis of a parametric resonance in the system is justified, a modification of the solution is found, and the appearance of processes with periods much longer than the fundamental oscillation period is demonstrated.

**DOI:** 10.1134/S1063772910110107

## 1. INTRODUCTION

Dynamo theory, which can explain the persistence of natural magnetic fields over time intervals far exceeding the characteristic decay times (see, e.g., [1]), is a nonlinear theory. In dynamo theory, the energy of thermal and radioactive sources and the energy released due to the differentiation of matter is converted into the energy of magnetic fields. Even the system describing convection is nonlinear. The inclusion of a magnetic field in the model can only increase the degree of nonlinearity, since the magnetic field affects the velocity field via the Lorentz force, which is quadratic in terms of the magnetic field. Even the simple Boussinesq model of thermal convection with a magnetic field contains four terms in which the temperature field,  $T$ , the velocity field,  $\mathbf{V}$ , and the magnetic field,  $\mathbf{B}$ , appear in products. This gives rise to extended field spectra, which can clearly be observed in many objects.

It is known from the general theory of nonlinear systems [2] that resonance instabilities can develop in multimodal models. Interest in such phenomena described by the dynamo theory has been maintained over many years, in particular, by “malfunction” effects in the dynamo action, which result in geomagnetic-field reversals and suggest explanations for the Maunder minimum in the context of the solar dynamo (see [3] for various scenarios of this phenomenon). Studies in this area prompted the recent numerical simulations [4–7], which demonstrated the development of instabilities in the process of magnetic-field generation by flows found by solving the full nonlinear dynamo system, including the back influence of the magnetic field on the flow. A small magnetic-field perturbation proves to be sufficient for the magnetic field to start growing exponentially.

This has been confirmed by many numerical simulations, from cascade models of turbulence to three-dimensional computations in planar or spherical geometries, which suggest the possibility of parametric resonances in such systems [8]. We will consider this phenomenon below using a Parker dynamo (frequently used in various areas of theory) as an example. The essence of our approach is to introduce a delay in the back influence of the magnetic field on the  $\alpha$  effect, which results in a parametric resonance in the system (such a delay was first suggested to account for variations in the cyclic character of solar activity in [9, 10]). In Section 2, we consider model equations and discuss the basis for this time delay. Section 3 considers the emergence of a parametric resonance in the system, the effect of the time lag on the behavior of the phase portrait of the system, and the variations in the phase shift between the poloidal and toroidal magnetic fields; we also show how the nonlinearity affects time changes in the shape of the curve. Section 4 presents a discussion of the results.

## 2. DYNAMO EQUATIONS

We consider Parker's dynamo model, which is frequently used to describe the generation of magnetic fields in galaxies, the solar dynamo, and the geodynamo [11, 12]. We will use the following thin-shell equations:

$$\frac{\partial A}{\partial t} = \alpha B + A'', \quad \frac{\partial B}{\partial t} = -\mathcal{D}A' + B'', \quad (1)$$

where  $A$  and  $B$  are the azimuthal component of the vector potential of the magnetic field ( $\mathbf{B} = \text{rot}\mathbf{A}$ ) and the azimuthal component of the magnetic field  $\mathbf{B}$ ;  $\alpha$  is the hydrodynamic helicity, which depends on the coordinate  $\vartheta$ ; and  $\mathcal{D}$  is the dynamo number, which is proportional to the product of the amplitudes of the

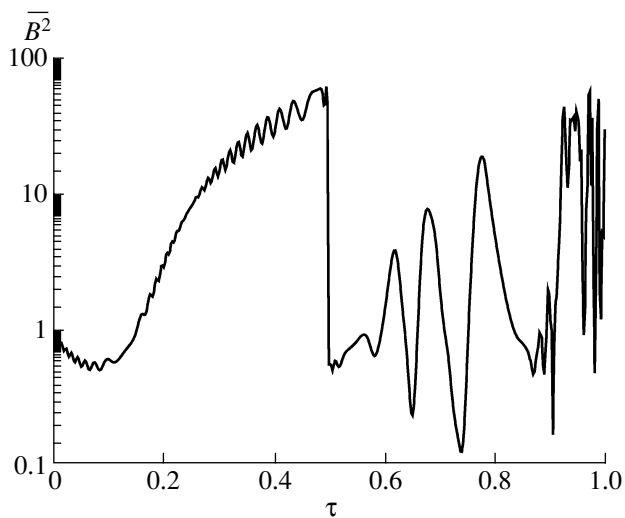


**Fig. 1.** The magnetic field  $B$  averaged over time and volume as a function of the time lag  $\tau$ . The field  $B$  is normalized so that  $B|_{\tau=0} = 1$ . The quantity  $\tau$  is measured in units of the period of  $B$  at  $\tau = 0$ .

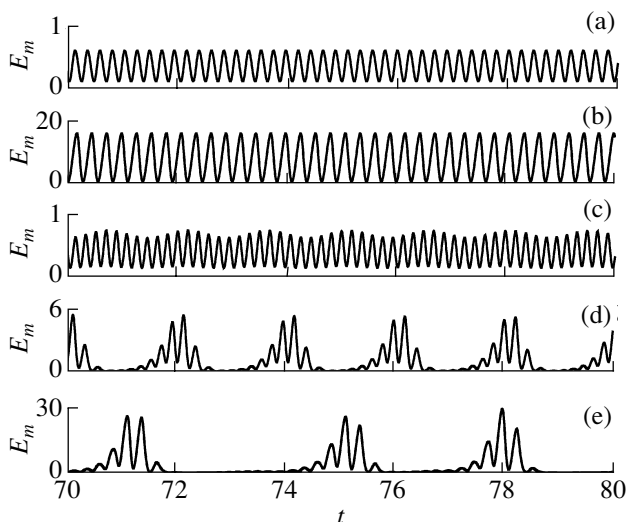


**Fig. 2.** Evolution of the volume-averaged magnetic energy for various time lags,  $\tau =$  (a) 0, (b) 0.33, (c) 0.57, (d) 0.67, and (e) 0.89.

$\hat{\alpha}$  and  $\hat{\omega}$  effects. A prime denotes a derivative with respect to  $\vartheta$ . At the boundaries of the region,  $\theta = \pm 1$  and the vacuum boundary conditions are satisfied,  $B = 0$  and  $A' = 0$ . We seek a solution in the form

$$(A, B) = e^{\gamma t}(\mathcal{A}(\vartheta), \mathcal{B}(\vartheta)). \quad (2)$$

The system (1) then reduces to the eigenvalue problem

$$\gamma \mathcal{A} = \alpha \mathcal{B} + \mathcal{A}'', \quad \gamma \mathcal{B} = -\mathcal{D} \mathcal{A}' + \mathcal{B}'', \quad (3)$$

where  $\gamma$  is the growth rate. According to the general representations, the pseudo-scalar quantity  $\alpha(\vartheta)$  is

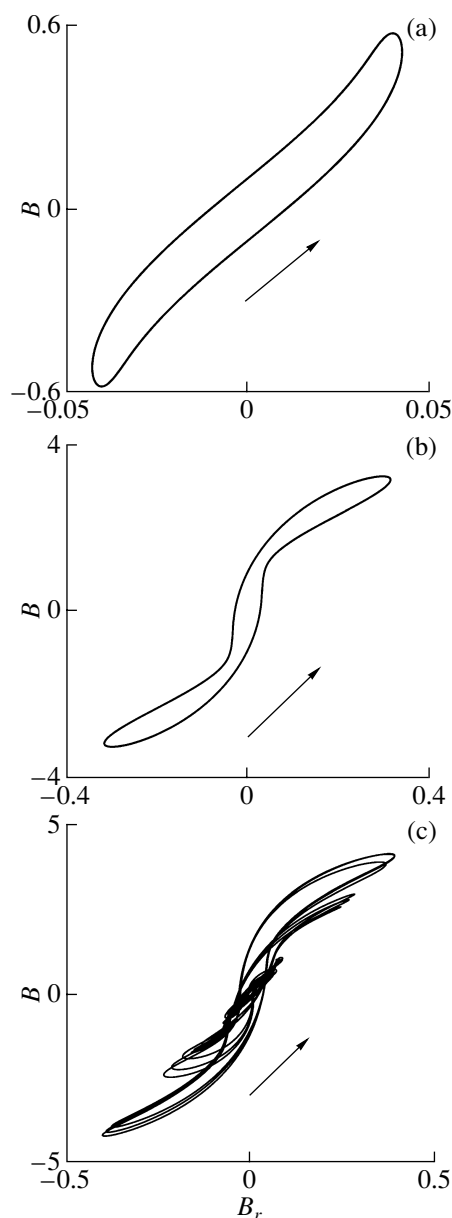


**Fig. 3.** Phase diagrams for various time lags,  $\tau =$  (a) 0, (b) 0.33, and (c) 0.89. The arrow corresponds to the direction of motion in phase space. The field values are taken at the point  $\vartheta = -0.9$ .

antisymmetric in  $\vartheta$  about to the equator:  $\alpha(-\vartheta) = -\alpha(\vartheta)$ . In this case, the solutions can be divided into two classes — quadrupolar (Q),  $\mathcal{A}(-\vartheta) = \mathcal{A}(\vartheta)$ ,  $\mathcal{B}(-\vartheta) = -\mathcal{B}(\vartheta)$ , and dipolar (D)  $\mathcal{A}(-\vartheta) = -\mathcal{A}(\vartheta)$ ,  $\mathcal{B}(-\vartheta) = \mathcal{B}(\vartheta)$ .

For  $\mathcal{D}_- < 0$ , the first mode ( $\mathcal{D}_-^{\text{cr}} \sim -8$ ) is quadrupolar and does not oscillate:  $\Im \gamma = 0$ . Typically, this regime is considered for the galactic dynamo, where the spatial dependence is associated with the disk-depth direction. For  $\mathcal{D} > 0$ , the first mode is dipolar and oscillates ( $\Im \gamma \neq 0$ ), while the excitation thresh-

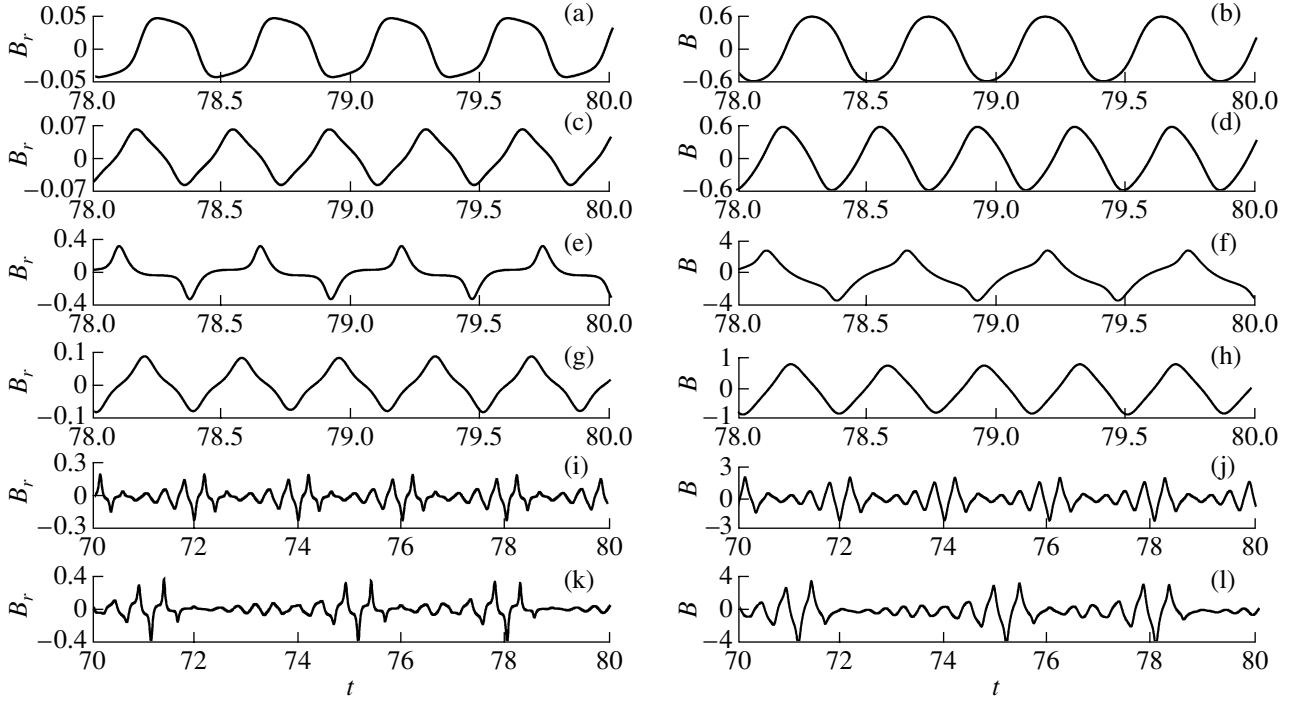


Fig. 4. Evolution of  $B_r$  (left) and  $B$  (right) for  $\tau = 0, 0.1, 0.33, 0.57, 0.67$ , and  $0.89$  (from top to bottom).

old is considerably higher,  $\mathcal{D}_+^{cr} \sim 200$ . We will further be interested precisely in this regime.

Introducing a nonlinearity of the form

$$\alpha(B) = \frac{\alpha_0(\vartheta)}{1 + B^2} \quad (4)$$

makes it possible to obtain quasi-stationary solutions without, on the whole, substantially changing the form of the eigenvalues of the system (3); see [13] for a comparison between the analytical and numerical results.

Generally, the nonlinearity (4) is not the only one possible. Among the important assumptions underlying (4) is that the response is instantaneous; this requires a strict justification. Currently, more complex models of  $\alpha$ -effect quenching due to the mean magnetic field are available, in which the evolution of the  $\alpha$  effect obeys a differential equation [14] and the characteristic relaxation time is close to the characteristic period of the field ( $A, B$ ). A substantial difference of our model from (4) is the possibility of a phase shift between  $\alpha$  and  $B$ . Based on a somewhat different dynamo equation describing the generation of the solar magnetic field, Yoshimura [10] showed that the delay of the Lorentz force relative to the magnetic field can give rise to long-period variations. The above studies mainly dealt with lags appreciably longer than the principal oscillation period (22 years). Obviously, introducing a long time lag necessarily results in the emergence of long-period disturbance. On the other

hand, physical reasons for the presence of such a long time lag are difficult to identify. We will show below that even a modest time lag can substantially modify the evolution pattern of the magnetic field in the Parker dynamo; we will also demonstrate a close relationship between this phenomenon and the parametric resonance.

### 3. PARAMETRIC RESONANCE

Since  $\alpha$  is a parameter of the system (1), we expect the emergence of a parametric resonance in the system. We consider here how the time lag  $\tau$  in the dependence

$$\alpha(\vartheta, t, \tau) = \frac{\alpha_0(\vartheta)}{1 + B^2(\vartheta, t - \tau)}. \quad (5)$$

affects the generation process. The calculations for  $\alpha_0 = \sin(\pi\vartheta)$  and  $\mathcal{D} = 300$  are illustrated in Fig. 1. The result is completely unexpected: although  $\alpha$  depends on  $B$  squared, the behavior of the mean magnetic-field energy is not symmetric with respect to  $\tau = 0.5$  (in units of the period of the process,  $T_0 \approx 0.45$ ). Thus, upon slightly reducing the magnetic-field amplitude, at  $0 < \tau < \tau_{\min} = 0.17$ , the magnetic field begins to grow sharply, remaining time-periodic (Fig. 2). At  $\tau = \tau_{br} \approx 0.5$ , the oscillation amplitude decreases abruptly (Fig. 2c) to its values at  $\tau_{\min}$ , and the amplitude becomes modulated with a new oscillation, whose period exceeds the oscillation period at

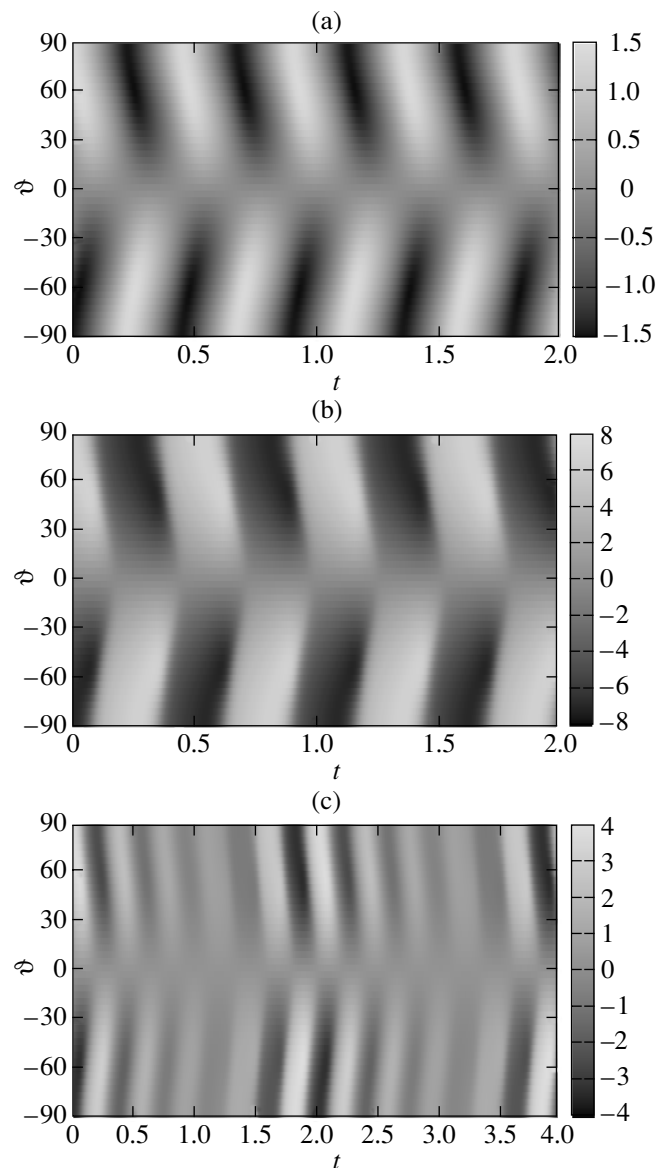


Fig. 5. Butterfly diagrams  $B(t, \theta)$  for  $\tau =$  (a) 0, (b) 0.33, and (c) 0.67.

$\tau = 0$  by a factor of eight for energy or a factor of four for the field. The amplitude of this oscillation increases with  $\tau$  (Figs 2d, 2e). Note that the period of the new oscillation begins varying at  $\tau = 0.89$  (Fig. 2e).

It is interesting to consider the phase diagrams in the variables  $(B_r, B)$ , where  $B_r = -A'_\theta$  is the radial (poloidal) component of the magnetic field. At  $\tau = 0$ , the behavior of the curve is regular, and the curve is nearly elliptical (Fig. 3a). The major-to-minor axis ratio is much greater than unity, which corresponds to a small phase of the shift between the field components,  $\varphi_{B_r, B} (= \varphi_{B_r} - \varphi_B)$ : the phase of the  $B_r$  components slightly lags  $\varphi_B$ . In the regions of the largest departures,  $B_r \approx \pm 0.05$ , an area with  $\beta = \frac{\partial B}{\partial B_r} \rightarrow$

$\pm\infty$  appears; it is slightly elongated in the direction  $B_r = \text{const}$ . Let  $B_r = \sin t$ ,  $B = \sin(t + \varphi_{B_r, B})$ ; then  $\beta \sim -\sin(\varphi_{B_r, B}) \text{tg } t$ . At  $\varphi_{B_r, B} < 0$ , the maximum value of  $\beta$  is within the region of the maximum  $B_r$  values, which can be seen in Fig. 3a.

Increasing  $\tau$  to 0.1 changes the shapes of the  $B_r$  and  $B$  curves from sinusoidal to sawtoothed (Fig. 4); this is first accompanied by a small increase in the time lag of  $B_r$  relative to  $B$  and then, with further increase in  $\tau$ , by phase equalization ( $\varphi_{B_r, B} \approx 0$ ). Increasing  $\tau$  to 0.33 results in manifestations of a parametric resonance, which appears as a growth of the magnetic-field amplitude and the emergence of a small peaked extremum. In Fig. 3b, a region of large  $|\beta|$  at small  $|B_r|$  and two regions of small  $|\beta|$  at large

$|B_r|$  can clearly be seen. All three regions exhibit a linear  $B(B_r)$  dependence.

The transition to  $\tau > 0.5$  is accompanied by a drop of the field amplitude (Figs. 1, 2, 4). To first approximation, the situation resembles the  $\tau = 0.1$  case (Figs. 1, 4). However, as is mentioned above, the emergence of a new long-period component (Fig. 2c) can already be distinguished. Note that such behavior was achieved in [10] for a time lag exceeding the principal period (see [3] for a survey of other mechanisms). Further increases in  $\tau$  result in the excitation of two oscillations, which can clearly be seen in the  $B(B_r)$  graph (Fig. 3c). The amplitude of the phase-shift oscillations  $\varphi_{B_r B} < 0$  increases with  $\tau$ .

Differences in the behavior of  $\overline{E_m}$  at  $0 < \tau < 0.5$  and  $0.5 < \tau < 1$  can be attributed to the accumulation of perturbations, which results in the development of instability. This is supported by an analysis of the solution for  $\tau > 1$ , which reveals a pattern similar to that in the region of  $0.5 < \tau < 1$ .

Up to now, we have not considered the dependence of the solution on  $\vartheta$  (from here on, we will assume that  $\vartheta$  varies from  $-\frac{\pi}{2}$  to  $\frac{\pi}{2}$ ). The dipolar solution represents a wave traveling from the poles to the equator, with a maximum field value at middle latitudes at  $\tau = 0$  (Fig. 5). Increases in  $\tau$  result in a transition to a solution with a stripey structure, i.e., to sharper polarity reversals in time and enhancements of the magnetic field at the poles (Fig. 5b). Further increases in  $\tau$  give rise to a periodicity with a longer period (Fig. 5c).

To confirm the parametric-resonance hypothesis, we consider a solution in the form of waves,  $B = b \sin(\vartheta - t)$ ,  $A = \sin(\vartheta - t + \varphi)$  and  $\alpha = \frac{1}{1+B^2(t-\tau)}$ . The equation for  $B$  does not explicitly include  $\tau$ ; for this reason, we consider only the equation for  $A$ . Multiplying the equation for  $A$  by  $A$  and integrating over the period yields  $\delta A(\varphi, \tau) = \alpha_0 \int_0^{2\pi} \frac{BA}{1+B^2(t-\tau)} dt$ . If  $|\Pi| > 1$ , where  $\Pi = \frac{\delta A(\varphi, \tau)}{\delta A(\varphi, 0)}$ , then the solution  $(A, B)$  is unstable.

The expression for  $\delta A$  has the form

$$\delta A(\varphi, \tau) = h_1 + h_2 \operatorname{tg} \varphi, \tag{6}$$

$$h_1 \approx 1 - 0.3 \cos \tau^2, \quad h_2 \approx 0.8 \sin(2\tau).$$

Then

$$\Pi = 1 + \frac{0.8 \sin(2\tau)}{1 - 0.3 \cos \tau^2} \operatorname{tg} \varphi, \tag{7}$$

and, for  $\varphi \rightarrow \pm \frac{\pi}{2}$  (which corresponds to  $\varphi_{B_r B} \approx 0$ ) and  $\tau \neq 0$ , the quantity  $|\Pi|$  increases (Fig. 6). Note that the curves are antisymmetric about the straight

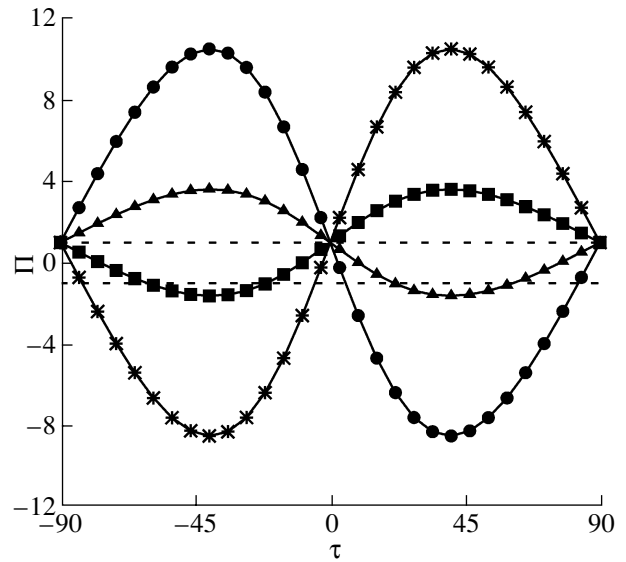


Fig. 6. Dependence  $\Pi(\tau)$  for various  $\varphi$  values:  $\varphi = 85^\circ$  (circles),  $70^\circ$  (triangles),  $-70^\circ$  (squares), and  $-85^\circ$  (asterisks); the dashed lines correspond to  $\Pi = \pm 1$ .

line  $\Pi = 1$ , i.e.,  $|\Pi(-t)| \neq |\Pi(t)|$ ; however, as the numerical simulations show, the increase of  $\varphi$  with  $\tau$  affects the stability more strongly due to the breakdown of the periodicity of the process. We will not consider this symmetry violation below.

#### 4. DISCUSSION

We have considered the dependence of the solution on the time lag for only one fixed dynamo number, as the  $\alpha$  effect is quenched by the magnetic field. Nevertheless, our analysis has revealed many new effects, such as a modification of the shapes of the evolution curves for the poloidal and toroidal magnetic fields, the emergence of zones of reduced and increased fields, and an instantaneous response in the  $\alpha$ -effect quenching. The observed enhancement of the field is due to the developing parametric resonance, since  $\alpha$  is a parameter in the equation for the poloidal component of the magnetic field. This does not contradict the simple analysis presented above. Another interesting finding is the emergence of an oscillation with a period much longer than the fundamental oscillation period, even for small time lags  $\tau$ . It would be interesting to compare the emergence of this periodicity with observationally known solar-activity periods that exceeding the basic 22-year period by factors of a few. The difficulty is understanding why the solution should be near  $\tau \approx 0.57$ . It is possible that more complex models with  $\tau$  found from the solution of the equations would demonstrate the presence of an attractor in this region.

## ACKNOWLEDGMENTS

I am grateful to D.D. Sokoloff for fruitful discussions.

## REFERENCES

1. Ya. B. Zeldovich, A. A. Ruzmaikin, and D. D. Sokoloff, *Magnetic Fields in Astrophysics* (Gordon Breach, New York, 1983).
2. L. D. Landau and E. M. Lifshitz, *Course of Theoretical Physics*, Vol. 1: *Mechanics* (Nauka, Moscow, 1982; Pergamon Press, New York, 1988).
3. S. M. Tobias, *Astron. Nachr.* **323**, 417 (2002).
4. F. Cattaneo and S. M. Tobias, *J. Fluid Mech.* **621**, 205 (2009); arXiv:0809.1801 [astro-ph] (2008).
5. A. Tilgner, *Phys. Rev. Lett.* **100**, 128501 (2008).
6. A. Tilgner and A. Brandenburg, *Mon. Not. R. Astron. Soc.* **391**, 1477 (2008); arXiv:0808.2141 [astro-ph] (2008).
7. M. Schrunner, D. Schmidt, R. Cameron, and P. Hoyng, *Geophys. J. Intern.* (2009, in press); arXiv:0909.2181 [astro-ph] (2009).
8. M. Reshetnyak, *Mon. Not. R. Astron. Soc.* (2010, in press); arXiv:1001.4234v1 [astro-ph] (2010).
9. H. Yoshimura, *Astrophys. J.* **221**, 1088 (1978).
10. H. Yoshimura, *Astrophys. J.* **226**, 706 (1978).
11. E. N. Parker, *Astrophys. J.* **122**, 293 (1955).
12. A. A. Ruzmaikin, D. D. Sokoloff, and A. M. Shukurov, *Magnetic Fields of Galaxies* (Nauka, Moscow, 1988; Kluwer, Dordrecht, 1988).
13. A. P. Bassom, K. M. Kuzanyan, and A. M. Soward, *Proc. R. Soc. London A* **455**, 1443 (1999).
14. N. I. Kleeorin and A. A. Ruzmaikin, *Magnetohydrodyn.* **18**, 116 (1982).

*Translated by A. Getling*